

Basic Investigations of Electrostatic Turbulence and its Interaction with Plasma and Suprathermal Ions in a Simple Magnetized Toroidal Plasma

A. Fasoli, F. Avino, A. Bovet, I. Furno, K. Gustafson, J. Loizu, P. Ricci, C. Theiler

Ecole Polytechnique Fédérale de Lausanne (EPFL), Centre de Recherches en Physique des Plasmas, Association EURATOM-Confédération Suisse, CH-1015 Lausanne, Switzerland

M. Spolaore, N. Vianello

Consorzio RFX, Associazione Euratom-ENEA sulla Fusione, Corso Stati Uniti 4, 35127

Padova, Italy

Email contact of main author: ambrogio.fasoli@epfl.ch

1. Introduction

Progress in understanding basic aspects of turbulence, its development from linearly unstable electrostatic modes, the formation of filamentary structures, or blobs, and its influence on the transport of energy and particles, both of the plasma bulk and of suprathermal components, can be achieved in a simple magnetized toroidal (SMT) device. Such configuration is obtained in the TORPEX device by combining a microwave plasma production scheme, creating weakly collisional plasmas of various gases characterised by pressure gradients, with a quasi-equilibrium generated by a toroidal magnetic field onto which a small vertical component is superimposed. The helical geometry of the open field lines, with magnetic field gradient and curvature, and electron temperatures in the eV range make these plasmas simplified paradigms of tokamak scrape-off-layer (SOL). Control parameters such as the background pressure, the power of the microwave source at 2.45GHz for plasma production, and the intensity of the vertical magnetic field can easily be varied to modify the plasma and turbulence characteristics [1].

In recent years, progress in blob physics has been very significant. After having clarified the formation of blobs in ideal interchange turbulence [2], TORPEX experiments elucidated the mechanisms behind the blob propagation, with a general scaling law relating their size and speed [3]. Such analytical scaling was verified over a wide range of the key dimensionless parameters in TORPEX data, vastly exceeding tokamak SOL databases, as well as in the results of 2D fluid numerical simulations [4-5]. During the past year, we have further consolidated the previous interpretation of blob motion using magnetic probe measurements of blob currents [6] and explored the insights gained from our previous studies to actively influence blob propagation in TORPEX [7]. In this paper, we summarise these two studies (Sections 2 and 3), after which we illustrate recent progress in the understanding of the interaction between suprathermal ions and turbulence (Section 4). We conclude with an outlook on future experiments (Section 5), focussed on the creation of a new configuration in TORPEX, in which magnetic surfaces are closed by a toroidal current driven in an in-vessel wire, allowing basic investigations of turbulence and of the associated plasma thermal and non-thermal response in the presence of magnetic configurations of increasing complexity and tokamak relevance.

2. Blob currents [6]

Obtaining direct local measurements of the parallel current density is a difficult challenge in thermonuclear plasmas. Various attempts are now in progress. In TORPEX, a specially designed current probe, consisting of an L-shaped array of 3 miniaturized three-axial pick up coils (3.5cm spaced, effective area of $2.3 \times 10^{-3} \text{m}^2$), was developed in collaboration with Consorzio RFX in Padova (I). Using this probe and conditional sampling techniques, 2D measurements of the parallel current density associated with radially propagating blobs were obtained. Figure 1 shows 2D profiles of the parallel current at three times during the blob propagation. An asymmetric dipolar structure of the current density is revealed, which originates from ∇B and curvature induced polarization of the blob and is consistent with sheath boundary conditions. The dipole is strongly asymmetric due to the non-linear dependence of the current density at the sheath edge upon the floating potential. Furthermore, by performing these measurements in hydrogen and helium plasmas we directly demonstrate the existence of separate regimes, in which currents damping blob motion are due to parallel conductivity and ion polarisation, respectively, compatible with the previously discovered scaling [3].

To investigate the effect of the observed asymmetry of the parallel current on the blob motion, we carried out numerical simulations of seeded blobs, using a two-field fluid model, which evolves electron density and vorticity [5]. The simulations span a wide range of blob sizes covering both regimes described above. We used either the complete or a linearized form for the sheath dissipation term in the vorticity equation. The structure of the parallel current density and plasma potential is found to be different in the two cases. Asymmetric profiles are observed in simulations with the complete form, while symmetric profiles are obtained when a linearized form is used.

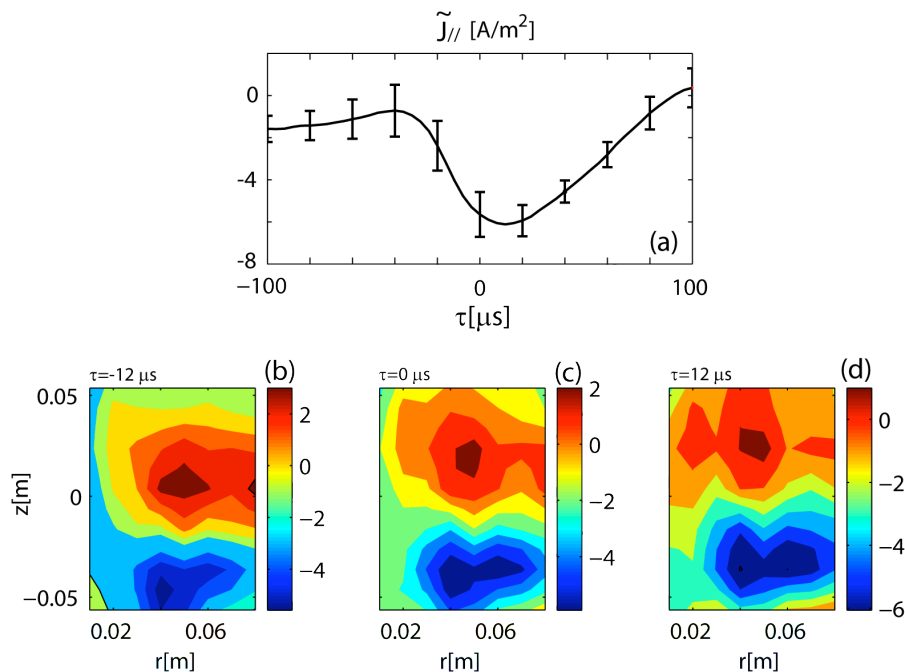


Fig. 1 Conditionally sampled data from the current probe measured $\sim 3\text{cm}$ in front of the limiter. Frame (a) shows an example time evolution of the parallel current density at $r=6\text{cm}$ and $z=-4\text{cm}$. Two-dimensional profiles of the parallel current density are shown at three different times during the blob radial propagation in frames (b-d).

3. Blob control and convective cells [7]

Based on our understanding of the physics governing blob motion, we have started to develop blob control methods. One of these methods, aimed at inducing radial flows and convective cells in the edge of tokamak plasmas, is based on the use of biased plates at the edge of the plasma. Basic principles of this idea have been tested in TORPEX [7]. A set of 24 electrodes has been installed on a metal limiter to modify the plasma potential and thus the cross-field flows in a controlled way. A sketch of this limiter is shown in Fig. 2 (top). The set of electrodes provides good flexibility. Different flow patterns are expected to be induced, such as convective cells, radially elongated flows, or vertical flows, as illustrated in the figure.

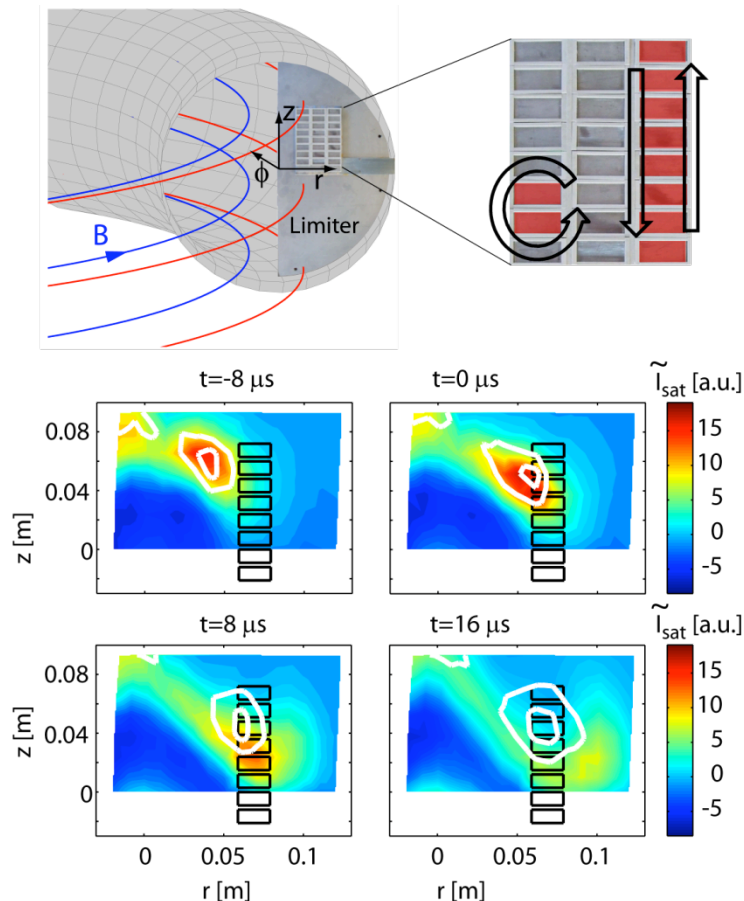


Fig. 2 Top: Sketch of the TORPEX vacuum vessel and the electrodes installed on a conducting limiter. Examples of magnetic field lines and the coordinate system are also shown. A zoomed in view of the electrodes is shown at the right. Shaded areas indicate examples of positively biased electrodes and arrows the expected flow pattern. Bottom: Conditionally averaged blob propagation (fluctuations in the ion saturation current) for the case where a vertical stripe of electrodes is biased to +40 V (color plots). For comparison, the white contours indicate the results of the same analysis when all electrodes are grounded.

Figure 2 (bottom) presents the effect on blobs, when a bias of +40 V is applied to the sets of electrodes indicated by black rectangles. Conditional average sampling is applied to obtain the average, 2D evolution of blob propagation. Successive time frames of blob propagation are obtained this way. Blobs are detected at the reference probe at $t=0$. In the same figure, the white contours depict the conditional sampled blob in the case without biasing. While early in time the average blob evolution is very similar, later on, as anticipated, the blob is swept strongly downwards due to the applied bias. The blob vertical velocity in the time window

$[-8\mu\text{s}, 8\mu\text{s}]$ is modified from ~ 700 m/s to ~ 2100 m/s due to the biasing, which also results in significant modifications of the time-averaged profiles. Measurements along and across the magnetic field show a fairly good toroidal symmetry of the changes induced by the biasing. Depending on the biasing scheme, radial and vertical blob velocities can be varied significantly. Due to a high level of cross-field currents, the magnitude of the achievable potential variations is well below the potential applied to the electrodes. In addition, the strongest potential variations are not induced along the biased flux tube, but at a position shifted in the direction of flows. Numerical simulations with a 2D drift-reduced Braginskii fluid code are in progress [5], in order to get insight into the mechanisms for these observed features, and possibly an idea of the limitations and extrapolability and of the proposed method to other devices.

4. Fast ion interactions with turbulence [8-10]

Suprathermal ion transport in plasma turbulence is another area in which experimental and theoretical studies based on basic plasma devices, including in the TORPEX SMT configuration, can contribute to understand basic burning plasma physics concepts. At macroscopic level, the transport of suprathermal ions in plasma is in general described by a diffusion equation. However, in the presence of high order terms associated with micro-scale processes, the transport process does not necessarily obey a diffusion equation. A useful micro-scale approach to describe the spreading of a population of an ensemble of suprathermal ions in general is the continuous time random walk [11]. This approach consists of following trajectories of random walkers through a sequence of steps. To quantify the dispersion of suprathermal ions one can define the variance of their radial displacement $\sigma_R^2 = \langle \delta R^2 \rangle$, and assume that its time evolution can be described by a power law $\sigma_R^2(t) \sim t^\gamma$. Here $\delta R = [R(t) - R(0)]$, and $\langle \rangle$ denotes an ensemble average over many particle trajectories. By numerically integrating the trajectories of suprathermal ions in simulated SMT turbulent fields, and by exploring wide ranges of particle energy and turbulence amplitude, we have shown that the ions have a complex motion, which in general cannot be considered diffusive [8]. The suprathermal ion dispersion starts with a brief ballistic phase followed by a turbulence interaction phase, which shows the entire spectrum of suprathermal ion spreading: super-diffusive ($\gamma > 1$), diffusive ($\gamma = 1$), or sub-diffusive ($\gamma < 1$), depending on particle energy and turbulence amplitude [9].

In Fig. 3 we illustrate three representative examples showing these three types of dispersion in the SMT: sub-diffusion at $E=250$, diffusion at $E=25$, and super-diffusion at $E=5$, where $E = mv_0^2/(2T_e)$ is the initial ion energy normalized to the plasma electron temperature. For these cases, the turbulence amplitude is such that $e\delta\psi/T_e \sim 0.8$, where $\delta\psi$ is the root mean square fluctuation amplitude of the electrostatic potential. The value of the exponent γ is determined by fitting the growth of σ_R^2 during the interaction regime with a power law. We follow 10^4 ion trajectories to satisfy statistical convergence with respect to the number of ions. We note that periodic oscillations in σ_R^2 are caused by the ion Larmor motion.

Following the ballistic phase, suprathermal ions interact with the plasma turbulence and the beam dispersion is characterised by a nearly constant γ . This quasi steady-state interaction phase ends when the ions have spread radially enough to sample regions where the local turbulent properties have changed significantly with respect to the injection position. Thus, the duration of the interaction phase is determined by the spread in the radial $E \times B$ velocity compared to the width of a roughly uniform region of turbulence.

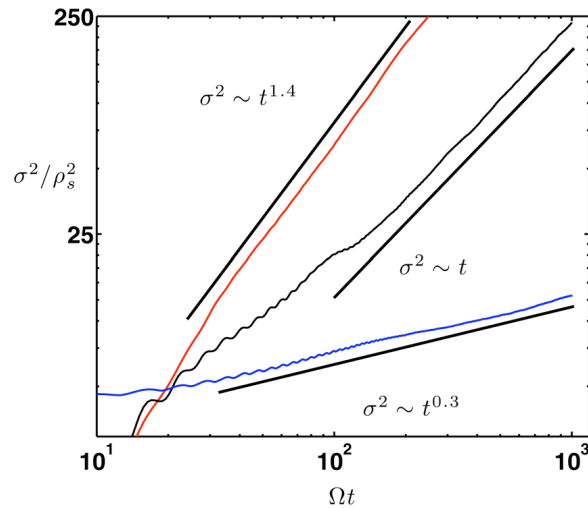


Fig. 3 Three representative examples of dispersion of a fast ion beam in TORPEX, expressed as the variance of the radial displacement as a function of time, in the presence of electrostatic interchange turbulence, showing sub-diffusion, diffusion, and super-diffusion.

In summary, our simulations show that the diffusion approximation is valid only locally, since γ can be drastically different than unity, and time-dependent. Therefore, the effective local suprathermal ion diffusivity can strongly depend on time, and can be two orders of magnitude away from the thermal particle diffusivity computed for the ideal interchange mode [12].

Having introduced the theory for suprathermal ion transport in turbulent plasmas for the SMT configuration, we discuss here how it can be applied to the interpretation of TORPEX experimental data and show an exploratory comparison between experiments and simulations. Suprathermal Li^{6+} ions are injected using a miniaturized ion source, which consists of a thermionic emitter with a two-grid accelerating system in a boron-nitride casing (outer diameter of 8mm). Li^{6+} ion currents up to $10\mu\text{A}$ are obtained. The source is mounted on a motorized movable system and can be continuously moved over a toroidal distance of 50cm (Fig. 4) [10].



Fig. 4 Lay-out and picture of the system allowing the fast ion source to be moved toroidally.

Ion energy and current density profiles are measured using a miniaturized gridded energy analyzer (GEA), which consists of two identical GEAs facing opposite directions for background noise subtraction. Each detector has small dimensions (15mm in diameter, 70mm in length and in inlet diameter of 8mm), and is able to measure fast ion currents as small as

0.1 μ A. Synchronous detection is used to increase the signal-to-noise ratio by modulating the emitter bias voltage at a given frequency (\sim 1kHz). The GEA detector is installed on a two-dimensional moving system, which allows reconstructing the ion current density profile with a spatial precision of 5mm over almost the entire poloidal cross section.

In the series of experiments described here, Li⁶⁺ ions with energy of \sim 70eV are injected horizontally in the blob region. The time average electron density at the injection location is \sim 5 \times 10¹⁵m⁻³ and the standard deviation of the floating potential time series, indicating the level of fluctuations, is \sim 1V. The ion source is moved toroidally between each discharge over a total distance of 50cm and poloidal profiles of the fast ion current are reconstructed at each toroidal position. Fig. 5 (left) shows an example of a fast ion current density profile at a toroidal distance of \sim 54cm from the source. The red cross indicates the position of the injection showing the displacement of the beam spot due to the vertical drift. Measurements are made with and without plasma, in the presence of magnetic fields and neutral filling gas. The radial and vertical spatial variances of the fast ion current profiles as a function of the toroidal angle are shown in Fig. 5 (right).

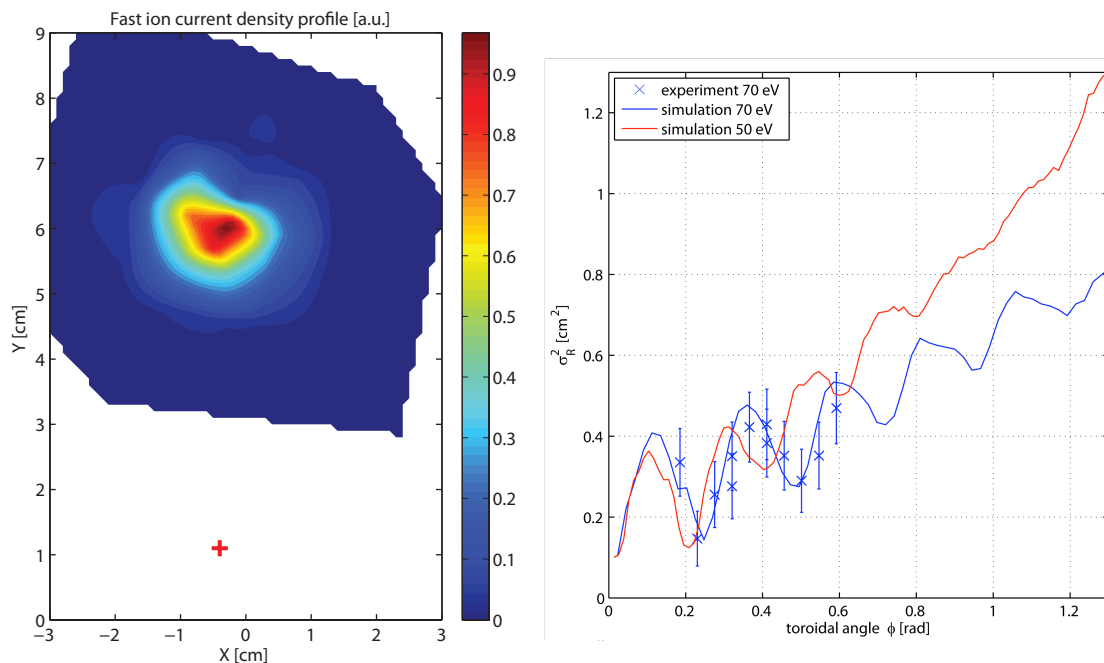


Fig. 5 Left: fast ion current density profile at a toroidal distance of 54cm from the source. Right: radial and vertical spatial variances of the fast ion current profiles as a function of the toroidal angle.

To interpret the experimental data, trajectories of tracer Li⁶⁺ ions are integrated in a turbulent electrostatic field resulting from the ideal interchange driven turbulence, which is calculated from 2D simulations of the drift reduced Braginskii fluid equations. Turbulence simulations are performed with different values of the particle and heat sources in order to match experimental profiles. At the injection point, the fluctuations level of the floating potential is higher in the simulation than in the experiment. In order to match the potential fluctuations, the simulated plasma potential fluctuations are rescaled. Using the simulated turbulent electric field, tracer Li⁶⁺ ion simulations are computed. Source parameters are based on measurements done without magnetic fields and 10000 particles are launched with initial parameters modelled with Gaussian distributions, with an energy of 70eV and a standard deviation σ of

10%. A synthetic diagnostic, mimicking the detector, computes 3D profiles of the fast ion current density for comparison with the experimental data [8,10]. Figure 5 displays, as a function of the toroidal direction, the variance of the beam profiles obtained with the synthetic diagnostic from the simulations, on top of the experimental measurements. The agreement is quite remarkable. The oscillations of the variance of the beam due to the Larmor motion of the particles are clearly evident. The broadening of the beam due to turbulence is revealed by the radial variance of the beam, which increases as a function of the distance from the source. Numerical simulations at later times indicate that, in these conditions, fast ions undergo a sub-diffusive transport with $\gamma \sim 0.78$. In the same figure, the variance of the beam profiles of simulated data for Li^{6+} energy of 50eV is also shown. They reveal a transition to a super-diffusive regime with $\gamma \sim 1.2$. Experimental measurements are ongoing to investigate this new regime.

5. Outlook: closing the flux surfaces with a current carrying internal wire

In its present setup, TORPEX can produce SMT configurations. To better mimic the scrape-off-layer and edge magnetic geometry of tokamaks, twisted field line configurations need to be created. To this aim, a copper wire running along the toroidal direction has been installed, in which a toroidal current can flow and generate a poloidal field. The twist of the magnetic field line is controlled by the amount of current driven in the wire. The wire is suspended inside the vacuum chamber through four insulated 1mm diameter stainless steel wires, visible in the picture shown in Fig. 7.



Fig. 7 The copper wire suspended inside TORPEX vacuum vessel

The wire is powered by a 1kA-10V power supply, whose output dynamics is limited to a maximum slew rate of $\sim 1400\text{A/sec}$. This allows reaching a maximum flat top current in approximately 300ms. For simplicity, water-cooling is used only for the portions of the conductors embedded in the coaxial feed-through. Therefore, the flat top current duration is limited by the Ohmic heating of the wire with almost pure radiative cooling in vacuum. A maximum current of $\sim 1000\text{A}$ should avoid overheating of the wire, thus allowing us to make ~ 100 discharges per day, with a flat top of approximately 400ms. The latter value will insure a data statistics similar to that in present SMT configurations. Preliminary measurements of the plasma properties in the presence of a toroidal current of the order of 600A-800A reveal significantly steeper pressure profiles than in the SMT configuration, and fluctuation spectra that are characterised by a skewness that undergoes a transition from positive to negative across the point of maximum gradient steepness.

The installation of the toroidal wire allows the production of magnetic geometries with single and double magnetic null-lines as well as, for particular combinations of currents in the existing set of poloidal coils, snowflake divertor configurations [13-14]. Some of these configurations are illustrated in Fig. 8. More complex geometries with multiple fully 3D X-points and/or magnetic ergodic/chaotic surfaces could also be generated by additional ad-hoc coils installed inside the TORPEX vessel. This system will allow basic investigations of the interaction of thermal plasma and suprathermal particles with instabilities and turbulence in magnetic configurations of increasing complexity, of more direct relevance to fusion.

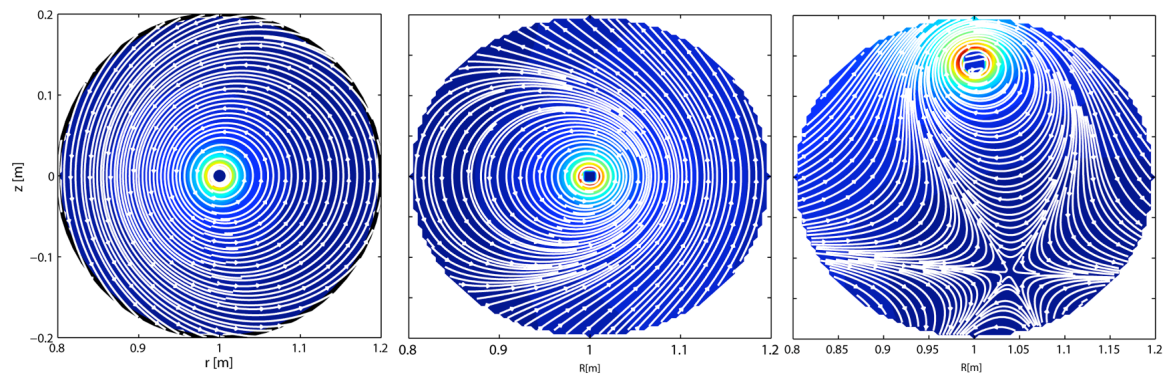


Fig. 8 Example of cross-sections of the various configurations that will be possible on the TORPEX configuration with internal wire, from limited, on the outboard or inboard side, to a snowflake-like divertor configurations.

This work was partly supported by the Fond National Suisse pour la Recherche Scientifique.

References

- [1] A. Fasoli et al., Plasma Phys. Control. Fusion 52, 124020 (2010).
- [2] I. Furno et al., Phys. Rev. Lett. 100, 055004 (2008).
- [3] C. Theiler et al., Phys. Rev. Lett. 103, 065001 (2009).
- [4] I. Furno et al., Plasma Phys. Control. Fusion 53, 124016 (2011).
- [5] P. Ricci et al., *this conference*.
- [6] I. Furno et al., Phys. Rev. Lett. 106, 245001 (2011).
- [7] C. Theiler et al., Phys. Rev. Lett. 108, 065005 (2012).
- [8] K. Gustafson et al., Phys. Plasmas 19, 062306 (2012).
- [9] K. Gustafson et al., Phys. Rev. Lett. 108, 035006 (2012).
- [10] A. Bovet et al., Nucl. Fusion 52, 094017 (2012).
- [11] E.W. Montroll and G.H. Weiss, J. Math. Phys. 6, 167 (1965).
- [12] P. Ricci and B.N. Rogers, Phys. Plasmas 16, 2303 (2009).
- [13] D.D. Ryutov, Phys. Plasmas 14, 064502 (2007).
- [14] F. Piras et al., Phys. Rev. Lett. 105, 155003 (2010).